Automatic Detection of Buried Mn-crust Layers Using a Sub-bottom Acoustic Probe from AUV Based Surveys

Umesh Neettiyath[1], Blair Thornton[2,1], Harumi Sugimatsu[1], Takayuki Sunaga[3], Junya Sakamoto[3], Hikari Hino[3]

[1]Institute of Industrial Science, The University of Tokyo, Komaba, 153-8505, Japan

(E-mail: umesh@iis.u-tokyo.ac.jp)

[2]Southampton Marine and Maritime Institute, University of Southampton, Southampton SO16 7QF, UK

[3]Japan Oil, Gas and Metals National Corporation, Toranomon, 105-0001, Japan

Abstract—A method for estimating the thickness of sediments covering buried layers of deep sea Cobalt-rich Manganese Crusts (Mn-crusts) from acoustic sub-bottom sonar data, recorded using an Autonomous Underwater Vehicle (AUV), is described. The acoustic data is analyzed with a combination of image and signal processing techniques to identify the optimal reflections coming from the seafloor and the buried layer. The method is applied to data collected from a field experiment and the results were validated using core samples from the same area; showing a high match. By including buried layers into volumetric estimation of Mn-crust deposits, resource potential of seafloor areas can be determined with better accuracy.

I. INTRODUCTION

Cobalt-rich manganese crusts (Mn-crust) as a seafloor deposit is increasing in prominence recently as it has high contents of valuable metals including Cobalt, Nickel, and rare earth elements [1]–[4]. These hydrogenetic deposits are formed mainly on the slopes and shoulders of seamounts ranging from 800m to 2400m [5]. The International Seabed Authority has assigned exploration slots to several countries for exploring these resources, and eventually exploiting them [6].

Different methods of surveying have been attempted by stakeholders with exploration rights and other researchers studying Mn-crusts. Physical sampling methods such as core drills or sampling from an ROV is useful for detailed analysis and confirmation of Mn-crusts [5], [7], [8]. Towed camera surveys are used for visual inspection to identify various seafloor types and the presence of exposed Mn-crust layers [9]. For large area resource estimation, ship based multibeam bathymetry and backscatter data are used together with other sensor data such as core samples, sub-bottom sonars, etc. [7], [10]–[12]. While sampling gives high accuracy thickness measurements with very low spatial resolution, multibeam and camera studies cannot measure thickness values. This became further complicated when buried Mn-crust layers were found below sediments, which cannot be seen in camera images. Thickness and coverage are important results necessary to estimate the volume of Mn-crust. In order to accurately estimate the complete resource potential, an integrated approach is necessary. Attempts to find the resource potential of seamount

scale areas by using multibeam backscatter data by verifying them with towed video surveys and sub-bottom profiler data is usually limited by the sparse thickness information collected by core sampling. In order to get continuous thickness information, an acoustic probe for in-situ contactless thickness measurement, and an underwater robot to conduct continuous surveys using the acoustic probe were developed by the Institute of Industrial Science of the University of Tokyo [13]. This system has been successfully deployed for Mn-crust volumetric surveys [14] and is being actively used. Similar acoustic probes were developed later by other researchers as well [15], [16].
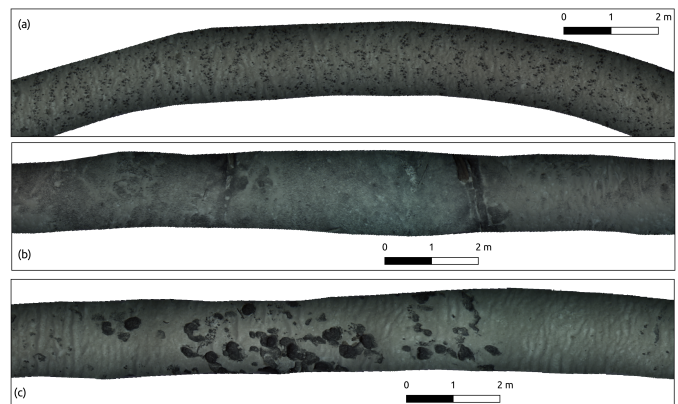
Fig. 1. Seafloor area mosaics from Mn-crust covered areas, mapped by AUV Boss-A. (a) nodule (and sediment) covered (b) exposed Mn-crust deposits (c) Mn-crust partially covered by sediments. This paper attempts to improve crust detection in mainly areas such as (c)

The proposed paper intends to expand the scope of the previous work [14] by considering buried crust layers. While the previous works focused on identifying and estimating exposed Mn-crust deposits, some sediment covered areas were found to be having layers below. Later studies found buried Mn-crust deposits in these areas. This research proposes an algorithm to calculate the thickness of these sediment deposits. By including shallow buried, potentially Mn-crust, layers along with the exposed Mn-crust deposits while estimating

crust coverage, more accurate volumetric distribution maps can be made. This method is particularly relevant for areas intermittently covered with sediments, an example of which is shown in figure 1(c).

Rest of this paper is organized as follows. A description of the AUV, the acoustic probe and other sensors used for survey are described in section II. Section III explains the algorithm developed for identifying the buried layers in the sediment and calculating its thickness. Section IV analyzes data collected during a field survey using the techniques proposed in section III and validates the results using core sample data. Conclusions and future work are presented in section V.

II. System Overview

The data is collected by an AUV, called Boss-A, built by the Institute of Industrial Science at the University of Tokyo for surveying Mn-crusts [17]. The AUV surveys the seafloor from an altitude of $\sim 1.5\,m$ using acoustic and visual sensors as shown in figure 2.

The acoustic system is based on a high power acoustic probe tuned for measuring Mn-crust thickness [13]. A $200\,kHz$ signal, modulated on a carrier signal of $2\,MHz$ is directed at the seafloor and the reflections are recorded. The recorded signal typically consists of reflections from the top of the seafloor and the bottom of the Mn-crust layer in crust covered areas. Whereas, in sediment covered areas, presence of a second reflection indicates a buried layer. The thickness can then be calculated by multiplying the time delay between the peak reflections with the velocity of sound in Mn-crust or sediment as appropriate.
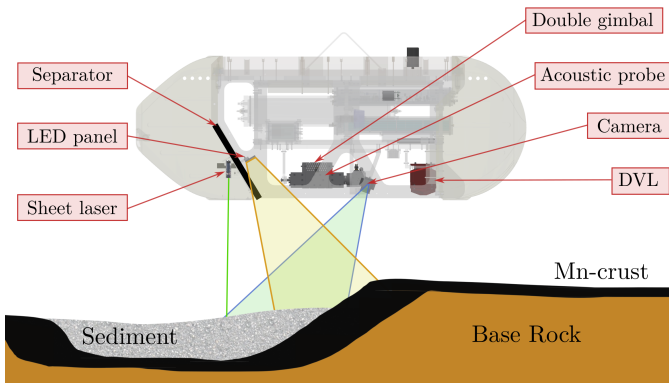
Fig. 2. Boss-A AUV measurement subsystems and components.

Since acoustic measurements are sensitive to the angle of incidence of the waves on the seafloor, the acoustic probe is mounted on a double gimbal mechanism which orients it normal to the seafloor [18]. This is done by calculating the orientation of the seafloor in real-time, using the data recorded by the visual system.

The visual system employs a light sectioning method to generate a 3D colour map of the seafloor using a sheet laser and a single camera and is based on [19]. The output of the system is a 3D colour point cloud of the seafloor with a swath $\sim 1.5\,m$ which is roughly equal to the survey altitude, and an across-track resolution of $\sim 1.4\,mm$ [14].

III. Methods and Workflow

The proposed algorithm builds upon the algorithm built by the authors in [14], [20], and follows the same concept of stacking adjacent recorded acoustic signals into an image frame and performing image analysis techniques, in addition to typical signal processing techniques to detect layers. The complete flowchart of the algorithm is given in figure 3.

The signals recorded by the acoustic probe, in the ideal case, consists of two reflections - one reflection from the top of the seafloor, i.e. the top of the Mn-crust or sediment layer, and one from the bottom of the layer. In deep sediment layers, beyond the penetration depth of the probe, which is $\sim 30\,cm$ as per the specifications, no secondary reflections will be present. However, in practice, the data is corrupted by noise arising due to scattering, multi-path reflections, and seafloor features such as local inclusions.

Initially, each received signal is analyzed individually to locate the reflection arising from the seafloor. The seafloor reflection is usually the strongest reflection. First, the envelope of the signal is extracted using Hilbert transform. A peak detection algorithm is then used to detect the local maxima in the signal. Then, the first peak having a sufficient signal to noise ratio (SNR) is selected as the seafloor reflection.

The major difference between detecting the bottom reflections of Mn-crust layers and the reflections from below the sediment layers is the intensity, continuity and spread of the signals. Mn-crust bottom reflections are sharper and can be detected using the intensity alone. However, in order to ensure the continuity of the thickness and remove noise from inclusions, a layer detection algorithm was developed [14]. In contrast, reflections from below the sediment layers are cluttered, spread over longer time periods and weaker. Also, there is considerable variation in reflections at different areas.

Therefore, in order to detect buried layers, a different analysis is performed. First, in order to remove shot noise, the signal data is initially filtered using a median filter. In order to obtain a high filtering performance, the resulting data is processed with a deconvolution based filter, denoted as *CSD Filter* in the flowchart shown in figure 3. Since deconvolution is highly sensitive to noise and noise levels are very high in underwater measurements, an equivalent operation was performed by calculating the cross spectral density (CSD) between the transmitted pulse and the received signal. The received signal is cropped using a moving rectangular window and the filter is applied. The signal is then filtered with a bandpass filter centred around the transmitted signal frequency of $200\,kHz$. The $3\,dB$ bandwidth of the result was calculated to be between $70\,kHz$ and $300\,kHz$ and a filtered pulse is

reconstructed by adding the filtered components, yielding a high signal to noise ratio.
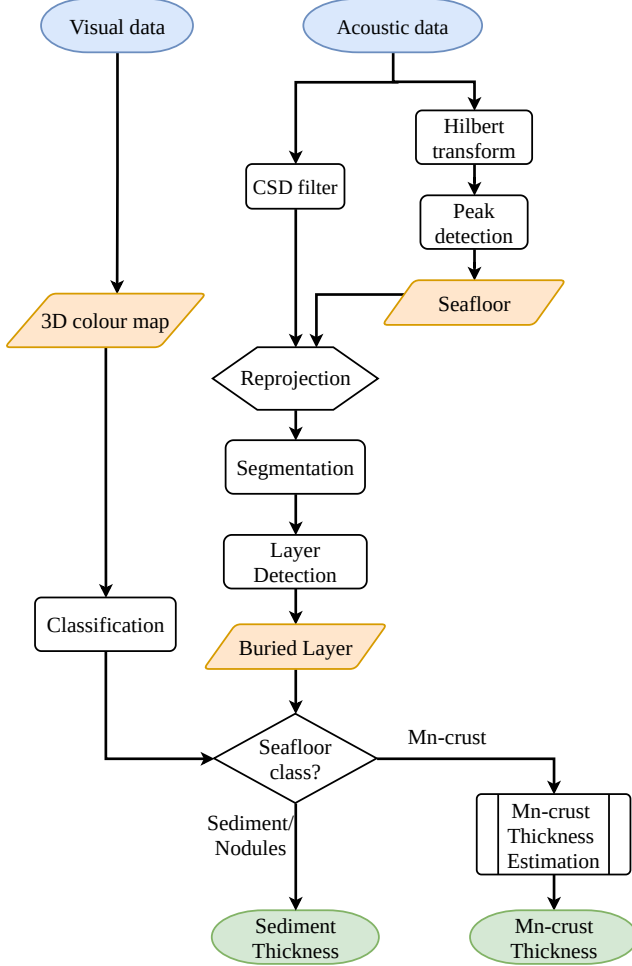
Fig. 3. Flowchart showing the analysis of AUV collected data to estimate the thickness of sediment deposits. The results at each stage of the acoustic data analysis is shown in figures 5 and 6

In the reprojection step, the CSD filtered acoustic data is projected into a distance-time axes using the seafloor location. The recorded data is represented on a time-time axes graph initially, with x-axis being the time when the signal was transmitted by the acoustic probe and y-axis being the time when the reflections were received by the probe. After reprojection, the x-axis is retained, but the y-axis is converted into a distance scale by multiplying the time with the speed of sound in sediment. This allows for easy visualization and analysis of the data with the goal of sediment thickness measurement. Also, only the relevant portion of the signal having strong reflections is retained and the rest are discarded. This is achieved by selecting the CSD filtered data around the seafloor location detected in the previous step and copying them into a new image frame.

The acoustic image reconstructed above has a horizontal resolution depending the speed of the AUV during the survey; in this case, the authors used a resolution of $0.01\,m$, which is the approximate average physical distance between two adjacent pulses when surveying at a speed of $0.2\,kn$. The vertical resolution was calculated using equation 1.

$$V_{res} = \frac{x_{shift} \cdot \nu_{sound}}{2 \cdot f_s} \tag{1}$$

where ν_{sound} is the velocity of sound in sediments, x_{shift} is the width by which the window is shifted while calculating the cross-correlation spectrum, and $f_s = 2\,\mathrm{MHz}$ is the rate of sampling of the measured signal. Although this vertical resolution does not accurately describe all parts of the image due to the change in speed of sound, it is valid throughout the sediment region of interest of the signal calculated in the previous step and thus can accurately describe the reflections inside the crust. In the example used in this paper, the vertical resolution was found to be $2.1\,mm$.

Since the areas of interest in the signal are continuous regions having relatively high intensity values, the signal is grouped into segments of equal width. Then, detection of the bottom layer is done using a signal intensity weighted integral function. For each segment and each potential thickness value, a cumulative signal level is calculated and the strongest cumulative sum is selected as the bottom layer. In sediment filled areas, this can be assumed to be the reflection originating from the buried layer.

A filtering is then performed to isolate areas covered with sediment or nodules and discard Mn-crust covered areas using seafloor classification data. 3D colour reconstruction of the seafloor, generated from the camera images recorded by the robot; is classified into Mn-crust, sediment or nodules by a machine learning algorithm using the method described in [14]; and is used for this purpose. Finally, a thickness estimate is made by multiplying the time difference with the speed of sound in sediment. A sound speed value of $\nu_{sound} = 1640\,\mathrm{m}/\mathrm{s}$ is used, which is calculated using the formula given by [21] for grain size values measured from the Mn-crust covered seamounts. The thickness of the Mn-crust is calculated separately using the previous method.

IV. RESULTS FROM FIELD SURVEYS

The proposed method is used to analyze a portion of the data collected by AUV Boss-A, during field deployments at an undisclosed location. Since core samples were also collected from this area by Japan Oil, Gas and Metals National Corporation (JOGMEC) using the Benthic Multi-coring System (BMS); this data was borrowed to validate the proposed method.

The seafloor patch which was analyzed is about $\sim 18\,m$ in length and $\sim 1.7\,m$ in width and lies at a depth of $\sim 1337\,m$. Figure 4 shows the 3D reconstruction of the surveyed area as top view and bathymetric map. Most of the seafloor is covered in sediments with rocky crusts projecting out in places, particularly in the middle and extreme right of the figure.
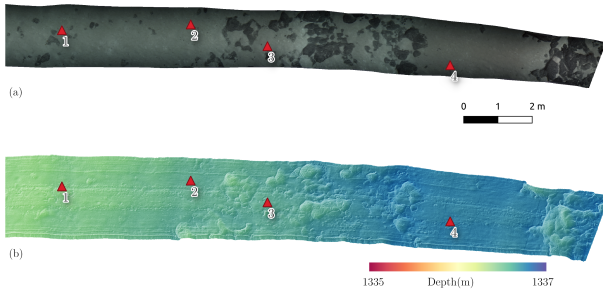
Fig. 4. (a) Top view of 3-D reconstruction (b) bathymetric map with hillshading of a seafloor patch $\sim 18\,m$ in length from the area surveyed by the AUV. This section contains mostly sediments with occasional rocks projecting out. Four of the samples from this area, collected using the BMS system, are used for validating the proposed algorithm. Their locations are shown as red triangles marked 1 to 4.
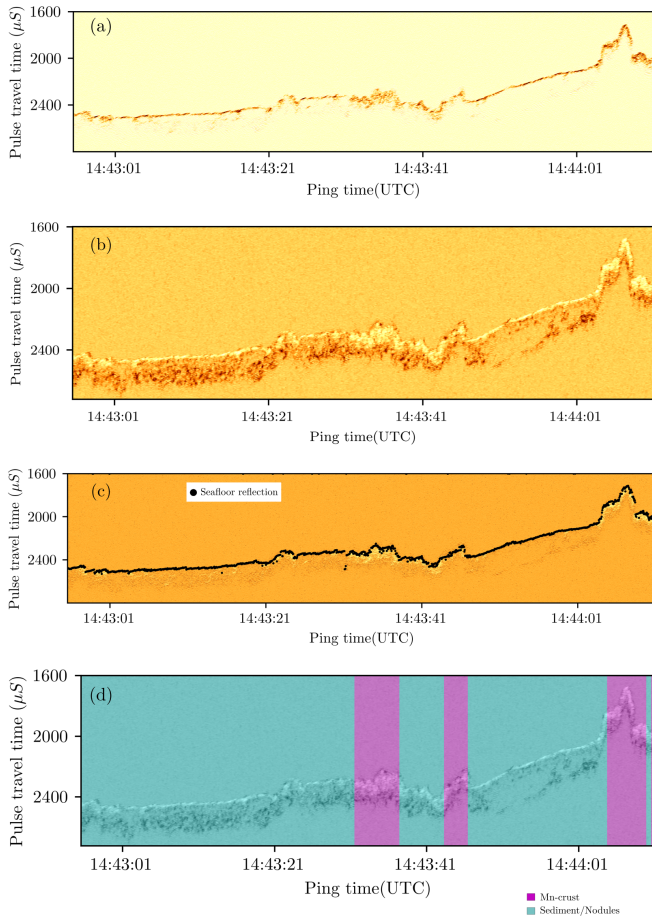
Fig. 5. Steps in analyzing the acoustic data corresponding to the seafloor patch shown in figure 4. (a) acoustic data recorded by the probe plotted on a logarithmic scale (b) processed signal after CSD filtering, showing the buried layer more clearly (c) the detected seafloor reflection, plotted over the Hilbert transformed acoustic data (d) seafloor classification, made from the 3D reconstruction, matched with the acoustic data.
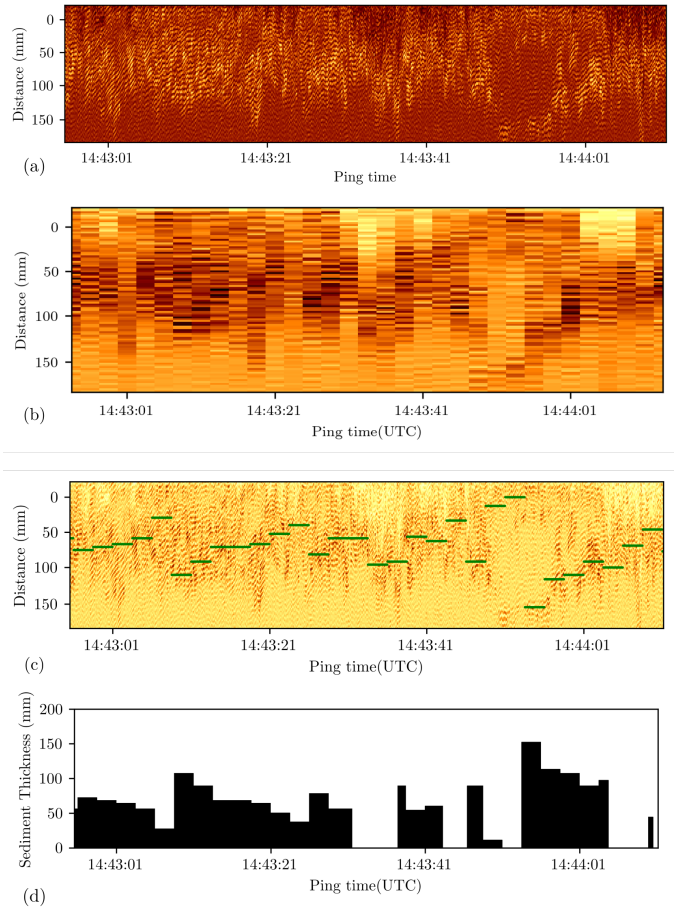
Fig. 6. Analysis steps leading up to the thickness of the sediment layer. (a) CSD filtered acoustic data aligned to the seafloor reflection. The seafloor is denoted as $0\,mm$ and distance is calculated w.r.to it (b) integrated intensity value for a segment width of $\sim 50\,cm$ (c) best thickness candidate for each segment, shown as a green line (d) estimated thickness of the sediment layer.

The acoustic data and the results at various stages of processing are shown in figures 5 and 6 . The raw acoustic data collected is shown in figure 5(a). Although it is plotted on a log scale, the buried layer reflections are not clearly visible. The resultant data after CSD filtering is shown in figure 5(b), which clearly shows the below sediment reflections. Figure 5(c) shows the Hilbert transformed signal and the detected seafloor reflections. Figure 5(d)shows the classification of seafloor made from the 3D reconstructions as a colour overlay over the corresponding acoustic signal.

The reprojected signals are shown in figure 6(a). The signal is segmented at a width of 50, which is approximately $50\,cm$ and the cumulative signal values are estimated as shown in and the final thickness values estimated are shown in figure 6(b). The segments having the strongest cumulative intensity is shown in figure 6(c), plotted as green lines over the reprojected signals. The final thickness estimate for the sediment deposit, filtered with the classification data, is plotted in figure 6(d).

A validation of the results was performed using core sam-

ples collected by the BMS from near the survey transect. Figure 7(a) shows the locations of the samples on the transect using red triangles. The locations of acoustic measurements made by Boss-A are shown using red dots in the same image. A total of 4 samples were used, with sediment cover varying from $6\,mm$ to $124\,mm$ in thickness. The Mn-crust layer on these samples was of the order of several tens of millimeters on Calcareous conglomerate substrate. The acoustic data is shown in figure 7(b); and the detected seafloor and buried layer reflections, along with the classification data are shown in figure 7(c). The calculated thickness values are plotted in figure 7(d) in black. The BMS measurements, mapped to the nearest thickness measurement are shown using red bars and the exact values are denoted above the figure.

It can be seen that samples 2,3 and 4 matches the thickness estimates closely, indicating the validity of the proposed method. Since the estimate is in steps, continuity of the thickness information is resolved into step size, which in turn depends on the segment width. A longer segment skips over continuous thickness variations, but is robust to noise such as local inclusions and signal level changes. The authors found that a value of $50\,cm$ provides a good balance.

There is a large difference between BMS1 ($6\,mm$) and the nearest thickness estimate ($70\,mm$). On close inspection, it can be seen that these two points are about $50\,cm$ away from each other. BMS1 is positioned between several exposed Mn-crust pieces, indicating that the sediment between them could be thin. Since the measurement point is further away, the sediment layer could be thicker. Also, the stronger filtering and amplification are performed to locate the below seafloor layers, makes it harder to identify the transition points where the exposed crust goes under the sediment deposits and becomes the buried layer. However, visual data which is collected along with the acoustic data can be used to detect these regions, but is out of scope of the present work.

While the proposed algorithm estimates the thickness of the sediment layer, it cannot identify the type of the buried layer or determine the thickness of the Mn-crust layer, if present. However, the sediment thickness in itself is valuable information and an estimate of the thickness can be interpolated from neighboring exposed Mn-crust areas, albeit less accuracy. Further verification of the proposed algorithm is planned using a testbench setup. Also, while the present study only analyzed a short section of the seafloor, the algorithm must be scaled to analyze the large volumes of data collected using the robot.

V. Conclusion

The authors proposed a method for detecting shallow buried layers of potential Mn-crust deposits in sub-bottom acoustic data collected by an AUV. This was achieved by stacking subsequent acoustic pulses into a frame and performing image and signal processing techniques to detect an optimal buried layer. The results were validated using core samples collected from near the surveyed area. Further validation is being planned by desk experiments. By incorporating potential Mn-crust layers below shallow sediments into the volumetric distribution estimates, in addition to exposed Mn-crust deposits, enhanced estimates of Mn-crust distribution can be made for large areas using autonomous robotic surveys, including past surveys.

References

[1] J. R. Hein, K. Mizell, A. Koschinsky, and T. A. Conrad, "Deep-ocean mineral deposits as a source of critical metals for high- and green-technology applications: Comparison with land-based resources," *Ore Geology Reviews*, vol. 51, pp. 1–14, jun 2013.

[2] M. R. Clark, R. Heydon, J. R. Hein, S. Petersen, A. Rowden, S. Smith, E. Baker, and Y. Beaudoin, *Deep Sea Minerals: Cobalt-rich Ferromanganese Crusts, a physical, biological, environmental, and technical review*, E. Baker and Y. Beaudoin, Eds. Secretariat of the Pacific Community, 2013.

[3] P. A. J. Lusty and B. J. Murton, "Deep-Ocean Mineral Deposits: Metal Resources and Windows into Earth Processes," *Elements*, vol. 14, no. 5, pp. 301–306, oct 2018.

[4] P. A. J. Lusty, J. R. Hein, and P. Josso, "Formation and Occurrence of Ferromanganese Crusts: Earth's Storehouse for Critical Metals," *Elements*, vol. 14, no. 5, pp. 313–318, oct 2018.

[5] A. Usui, K. Nishi, H. Sato, Y. Nakasato, B. Thornton, T. Kashiwabara, A. Tokumaru, A. Sakaguchi, K. Yamaoka, S. Kato, S. Nitahara, K. Suzuki, K. Iijima, and T. Urabe, "Continuous growth of hydrogenetic ferromanganese crusts since 17 Myr ago on Takuyo-Daigo Seamount, NW Pacific, at water depths of 800–5500 m," *Ore Geology Reviews*, vol. 87, pp. 71–87, jul 2017.

[6] International Seabed Authority, "Regulations on Prospecting and Exploration for Cobalt-rich Ferromanganese Crusts in the Area," 2012.

[7] B. Zhao, Y. Yang, X. Zhang, G. He, W. Lü, Y. Liu, Z. Wei, Y. Deng, and N. Huang, "Sedimentary characteristics based on sub-bottom profiling and the implications for mineralization of cobalt-rich ferromanganese crusts at Weijia Guyot, Western Pacific Ocean," *Deep Sea Research Part I: Oceanographic Research Papers*, vol. 158, p. 103223, apr 2020.

[8] K. Nishi, A. Usui, Y. Nakasato, and H. Yasuda, "Formation age of the dual structure and environmental change recorded in hydrogenetic ferromanganese crusts from Northwest and Central Pacific seamounts," *Ore Geology Reviews*, vol. 87, pp. 62–70, 2017.

[9] G. He, W. Ma, C. Song, S. Yang, B. Zhu, H. Yao, X. Jiang, and Y. Cheng, "Distribution characteristics of seamount cobalt-rich ferromanganese crusts and the determination of the size of areas for exploration and exploitation," *Acta Oceanologica Sinica*, vol. 30, no. 3, pp. 63–75, may 2011.

[10] J. Joo, S. S. Kim, J. W. Choi, S. J. Pak, Y. Ko, S. K. Son, J. W. Moon, and J. Kim, "Seabed mapping using shipboard multibeam acoustic data for assessing the spatial distribution of ferromanganese crusts on seamounts in the western pacific," *Minerals*, vol. 10, no. 2, pp. 1–20, 2020.

[11] D. Du, X. Ren, S. Yan, X. Shi, Y. Liu, and G. He, "An integrated method for the quantitative evaluation of mineral resources of cobalt-rich crusts on seamounts," *Ore Geology Reviews*, vol. 84, pp. 174–184, 2017.

[12] D. Du, C. Wang, X. Du, S. Yan, X. Ren, X. Shi, and J. R. Hein, "Distance-gradient-based variogram and Kriging to evaluate cobalt-rich crust deposits on seamounts," *Ore Geology Reviews*, vol. 84, pp. 218–227, 2017.

[13] B. Thornton, A. Asada, A. Bodenmann, M. Sangekar, and T. Ura, "Instruments and methods for acoustic and visual survey of manganese crusts," *IEEE Journal of Oceanic Engineering*, vol. 38, no. 1, pp. 186–203, jan 2013.

[14] U. Neettiyath, B. Thornton, M. Sangekar, Y. Nishida, K. Ishii, A. Bodenmann, T. Sato, T. Ura, and A. Asada, "Deep-Sea Robotic Survey and Data Processing Methods for Regional-Scale Estimation of Manganese Crust Distribution," *IEEE Journal of Oceanic Engineering*, vol. 46, no. 1, pp. 1–13, 2020.

[15] F. Hong, H. Feng, M. Huang, and B. Wang, "An effective method for measuring the thickness of Cobalt-rich Manganese Crust based on the neighborhood information and dual- channel information," in *23rd International Congress on Acoustics*, no. September, Aachen, Germany, 2019, pp. 4446–4453.

[16] Hong, Feng, Huang, Wang, and Xia, "China's First Demonstration of Cobalt-rich Manganese Crust Thickness Measurement in the Western Pacific with a Parametric Acoustic Probe," *Sensors*, vol. 19, no. 19, p. 4300, 2019.

[17] Y. Nishida, K. Nagahashi, T. Sato, A. Bodenmann, B. Thornton, A. Asada, and T. Ura, "Autonomous Underwater Vehicle "BOSS-A" for Acoustic and Visual Survey of Manganese Crusts," *Journal of Robotics and Mechatronics*, vol. 28, no. 1, pp. 91–94, feb 2016.

[18] T. Sato, B. Thornton, A. Bodenmann, A. Asada, and T. Ura, "Towards real-time control of a double gimbaled acoustic probe for measurement of manganese crusts thickness," in *2013 IEEE International Underwater Technology Symposium (UT)*. IEEE, mar 2013, pp. 1–5.

[19] A. Bodenmann, B. Thornton, and T. Ura, "Generation of High-resolution Three-dimensional Reconstructions of the Seafloor in Color using a Single Camera and Structured Light," *Journal of Field Robotics*, vol. 34, no. 5, pp. 833–851, dec 2017.

[20] U. Neettiyath, B. Thornton, M. Sangekar, K. Ishii, T. Sato, A. Bodenmann, and T. Ura, "Automatic Extraction of Thickness Information from Sub-Surface Acoustic Measurements of Manganese Crusts," in *Oceans 2017 - Aberdeen*. IEEE, jun 2017, pp. 1–7.

[21] K. Mizuno, A. Asada, F. Katase, K. Nagahashi, T. Ura, and T. Haraguchi, "Development of the Parametric Sub-Bottom Profiler for Autonomous Underwater Vehicles and the Application of Continuous Wavelet Transform for Sediment Layer Detections," *The Journal of the Marine Acoustics Society of Japan*, vol. 43, no. 4, pp. 233–248, 2016.
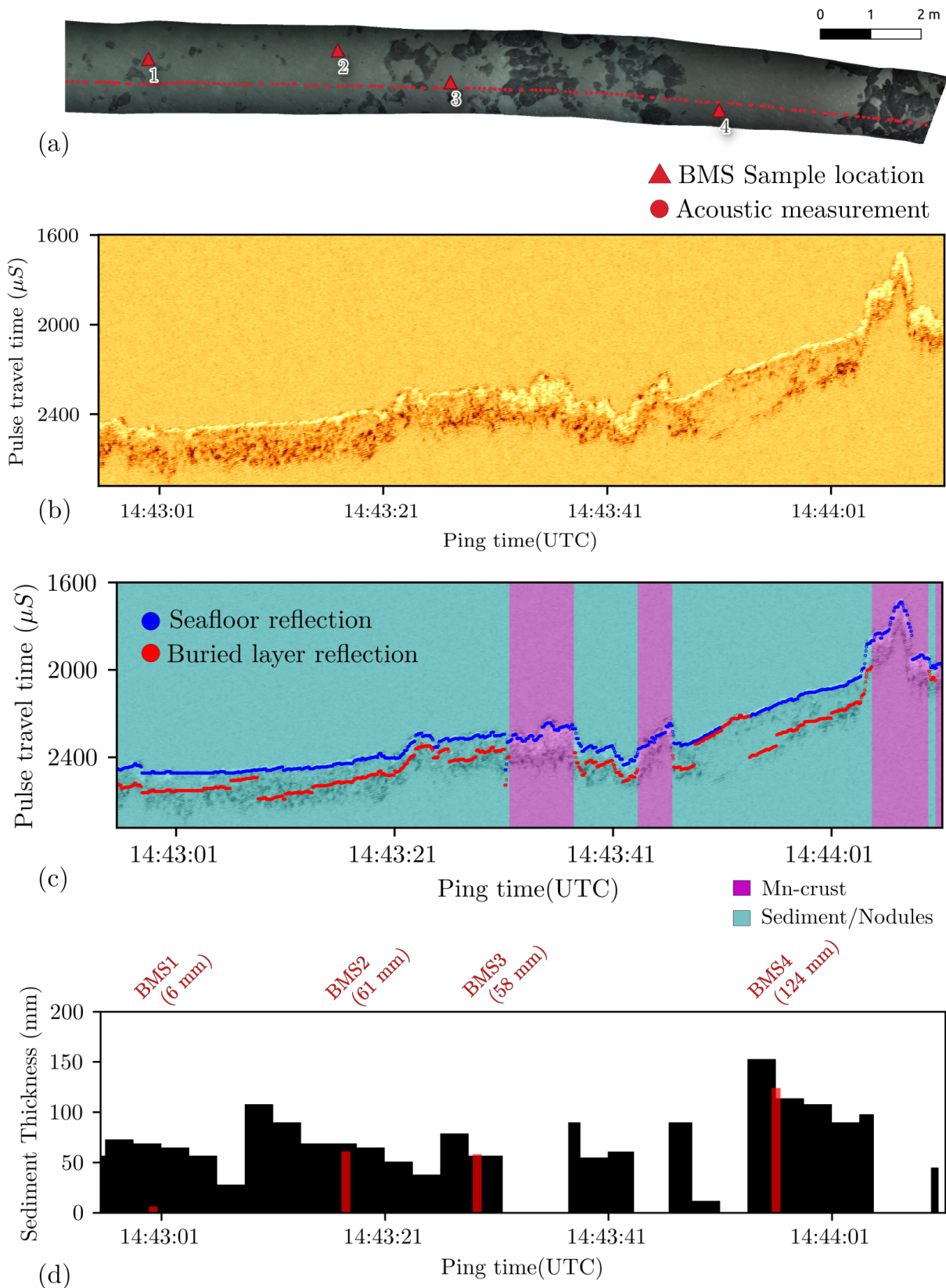
Fig. 7. Results and validation of the thickness estimates using samples collected by the BMS (a) 3D map (top view) of the area surveyed by AUV Boss-A showing the location of the acoustic measurements and BMS sampling locations (b) processed acoustic data from the area clearly showing buried layers (c)seafloor and buried layer detection plotted over the acoustic data and the seafloor classification data, made using the visual data (d) sediment thickness values estimated by the algorithm (black) compared with the thickness values measured by the BMS system (red). The exact BMS thickness values are noted above the figure. Mn-crust thickness values are not shown.